Geochemistry of Kapili Komatiite from Badampahar-Gorumahisani greenstone belt, Singhbhum craton, India and its resemblance with 'Barberton Komatiite'

Pawan Kumar Yadav* and Manorama Das
*Senior Geologist
Geological Survey of India,
SU: Bihar, Lohia Nagar, Kankarbagh, Patna-800020

Received Nov. 01, 2017 Accepted Dec. 09, 2017

ABSTRACT *The present study documents the field, petrographic and geochemical data on Kapili Komatiite from the Mesoarchaean Badampahar-Gorumahisani greenstone belt of the Singhbhum Craton, eastern Indian shield, and attempts to draw a comparison with similar history of sedimentation and volcanism in other contemporary Archaean greenstone belts of the world. Komatiite displays well preserved cumulate zone, platy and random spinifex zone. The studied komatiite contains olivine and pyroxene which are now altered to serpentine, secondary magnetite, tremolite, talc and chlorite. The komatiites are quite enriched in SiO_2 (38-47 wt%) and MgO (20-36 wt%), depleted in Al_2O_3 (2.51-6.75 wt%) and TiO_2 with significantly higher Al_2O_3/TiO_2, CaO/Al_2O_3, Sm/Nd, $(La/Sm)_N$, $(Gd/Yb)_N$ and $(La/Yb)_N$ ratios indicating affinity with Barberton Komatiite.*

Keywords: *Komatiite, Badampahar-Gorumahisani greenstone belt (BGGB), Iron Ore Group (IOG), Singhbhum Craton, India.*

Introduction

The high-MgO ultrabasic rocks, the komatiites occur mainly in Archean greenstone belts (Viljoen and Viljoen, 1969a; Arndt and Nisbet, 1982). These komatiites are reported from many other Archaean greenstone belts viz., Commondale, South Africa, 3.3Ga; Ball, Canada, 2.9Ga; Munro, Canada, 2.7Ga; and Tisdale, Canada, 2.7Ga. Komatiitic magma, being directly derived from high degree melting of mantle plumes (~30%), acts as a window which provides key information about composition and melting processes that operated in deep Archean mantle (Green, 1975; Ohtani et al., 1989; Xie et al., 1993; Boehler et al., 1995; Herzberg, 1995; Arndt, 2003 and Arndt et al., 2008). Allegre, 1982 and Arndt et al., 1998 proposed komatiitic magmas as product of peridotite partial melting, whereas, other consider the generation of komatiites by the wet and shallow melting of hot, depleted peridotite in the mantle wedge above a subduction zone (Grove and Parman, 2004).

There are many reported occurrences of komatiites from the Archaean Sargur schist belt of the Dharwar craton, southern India (Subba Rao and Naqvi, 1999; Jayananda et al., 2008; Tushipokla and Jayananda, 2013). Occurrences of komatiites from eastern Iron Ore Group (IOG) have been previously reported from Patharkata (Sahu and Mukherjee, 2001), Dhipasai (Chaudhuri et al., 2015), Kapili (Yadav et al., 2015; Yadav et al., 2016) and Tiring (Yadav and Das, 2017) villages situated in the Badampahar-Gorumahisani greenstone belt (BGGB), Singhbhum Craton. In this paper, we present petrographic, major oxides, trace elements and REE data of Kapili komatiite and compare our data with the Barberton komatiite, South Africa.

Geological Setting

The Palaeo-Mesoarchaean rocks in Singhbhum craton encircle the core of Archaean Singhbhum Granitoid (SG) batholiths (Fig.1). The oldest member of Singhbhum Craton comprises of a sequence of metasediments and metavolocanics called as Older Metamorphic Group (OMG) dated at ~3.5-3.6Ga (Saha, 1994; Mukhopadhyay, 2001; Misra et al., 1999; Misra, 2006). The OMG rocks are intruded by the TTG gneisses which are termed the Older Metamorphic Tonalite Gneiss (OMTG) and dated at 3.44Ga (Goswami et al., 1995). The Singhbhum Craton was subjected to several episodes of voluminous granitic plutonism of granodioritic to granitic composition known as Singhbhum Granite (Saha, 1994) during 3.3-3.1Ga. The central granitoid nucleus is flanked by three BIF bearing greenstone belts named as Eastern, Western and Southern Iron Ore Group of rocks (Fig.1). Supracrustals of the IOG comprising bimodal volcanic rocks, ultramafic rocks, banded iron formation (BIF), chert, shale and minor carbonates. Occurrence of komatiite near Kapili has been recorded in the BGGB as part of the Iron ore succession in the eastern IOG belt (Fig.1).

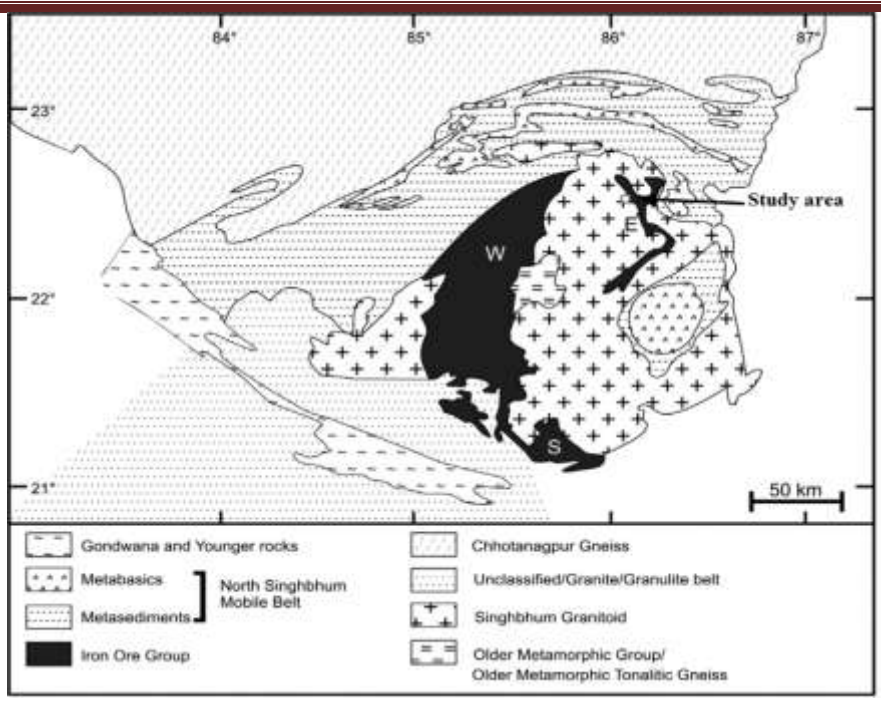

Fig.1: Outline geological map of the Singhbhum Craton, North Odisha, India (modified after Mukhopadhyay, 2001). The study area falls close to the boundary between the eastern Iron Ore Group of rocks and the Singhbhum Granite. E, W, S represents the eastern, western and southern Iron Ore belts respectively.

Geology of the study area

Komatiite occurrence was recorded from a small hillock (~800mX~500m) trending N30ºE-S30ºW near Kapili located in a NW-SE trending linear belt in the central part of the BGGB in Mayurbhanj district, Odisha (Fig.2). Komatiite shows concordant relationship with the metabasalt and talc-tremolite-serpentine schist. The komatiite of Kapili hill section display well preserved spinifex zone, (Fig.3a&b), platy zone (Fig.3c) and cumulate zone (Fig. 3d). At places, the cumulate zone shows prominent cooling cracks, filled with thin vein-lets of serpentine (Fig.3d). In the spinifex zone, the maximum dimension of olivine plate is ~20 cm although lengths of their long axes are mostly confined between 5 and 10cm (Fig.2a&b). Olivine plate size varying from 15-30 cm in length and 1-3 cm in width respectively in the platy zone. Primary minerals like olivine and pyroxenes are mostly altered to chlorite, tremolite, actinolite, epidote, talc, serpentine and magnetite indicating assemblage of greenschist to lower amphibolite facies of metamorphism.

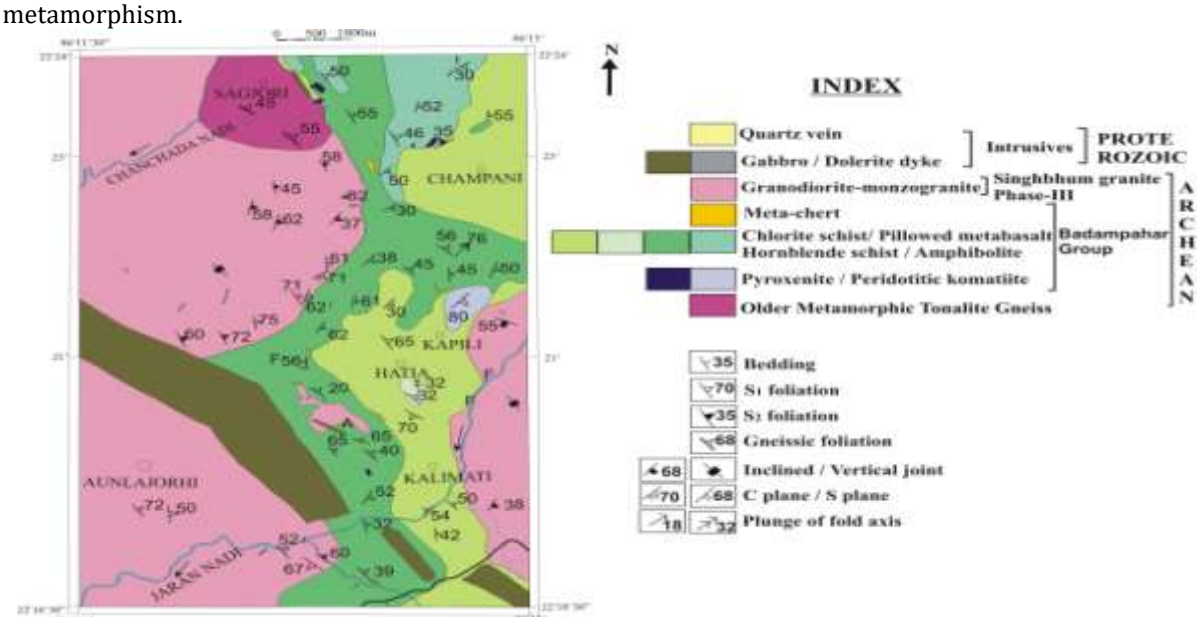

Fig.2: Geological map of the study area showing the occurrence of komatiite near Kapili.

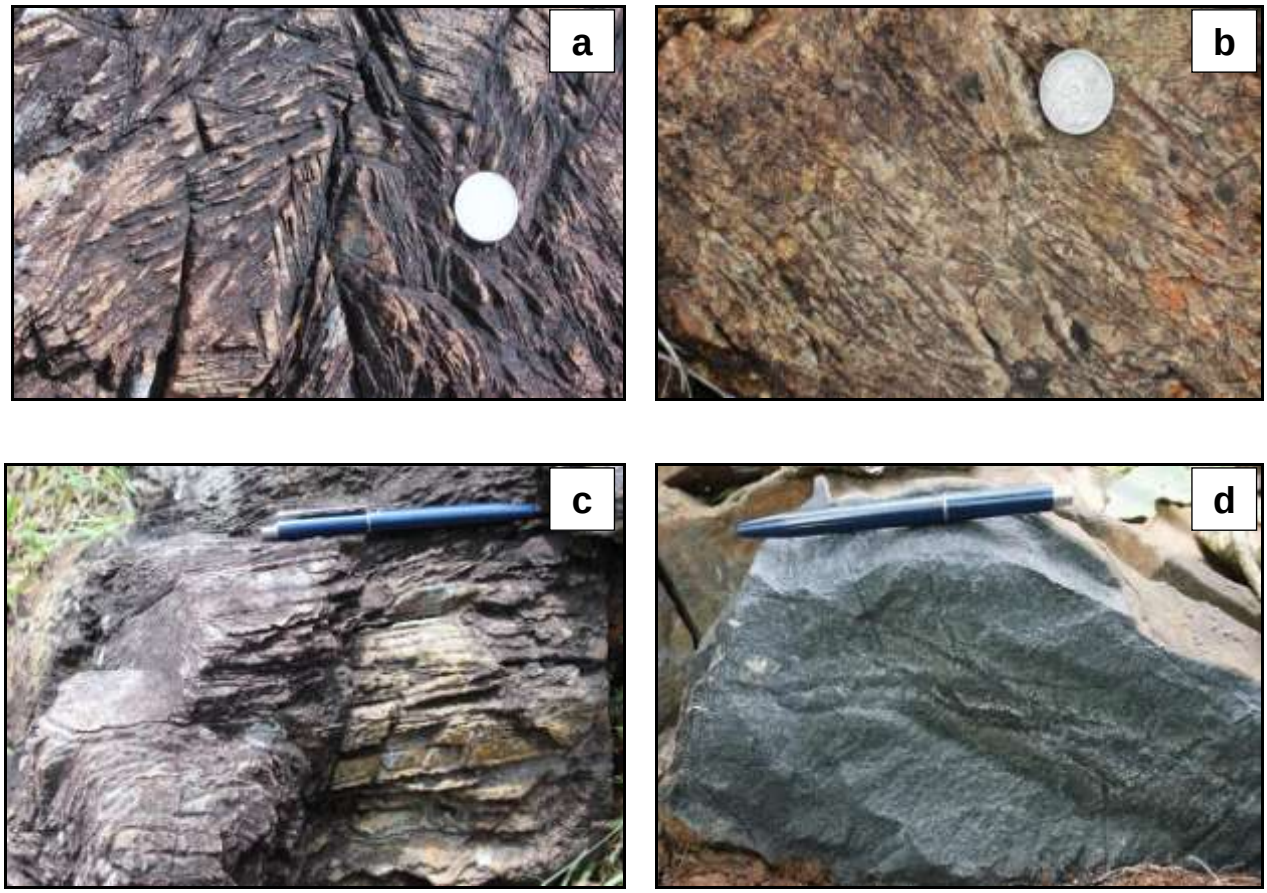

Fig.3: Field photographs **(a & b)** Random spinifex zone displaying network of randomly orientated olivine needles. **(c)** Platy spinifex zone consists of parallel arrangement of olivine and pyroxene plates. **(d)** Cumulate zone traversed by thin vein-lets of serpentine.

Mineralogy and texture of komatiites

Komatiites of Badampahar-Gorumahisani greenstone belt with MgO concentrations between 20-36% are metamorphosed to tremolite-serpentine-chlorite and tremolite-chlorite-talc schists. They contain the mineral assemblage olivine-serpentine-tremolite-chlorite-magnetite-talc ± clinopyroxene ± orthopyroxene ± pyrite. Spinifex zone of this rock consists of both random (Fig.4a&b) and platy spinifex (Fig.4c&d) textures. Spinifex texture is defined by the criss-cross arrangement of acicular primary minerals like olivine and pyroxenes, which are altered to serpentine, tremolite, chlorite and secondary magnetite (Fig.4a&b). Alternate plates of olivines and pyroxenes are also preserved within this zone. Olivine plates are replaced by serpentine and secondary magnetite whereas pyroxenes plates are mostly altered to tremolite (Fig.4c&d). Secondary magnetites are abundant and typically occur within the plates of olivine in feather-like shapes (Fig.4a). Chlorite, serpentine, magnetite and glass formed the matrix of this zone and are mostly anhedral in shape. The essential minerals of the cumulate zone are olivine pseudomorphed by serpentine and magnetite, clinopyroxene and tremolite. The cumulus phase is represented by pseudomorphic olivine (Fig.4e) and the intercumulus space is occupied by tremolite, serpentine, magnetite, chlorite and talc (Fig.4e). Arrested growths of incipient tremolite near the grain boundary of olivine are observed in some samples (Fig.4f).

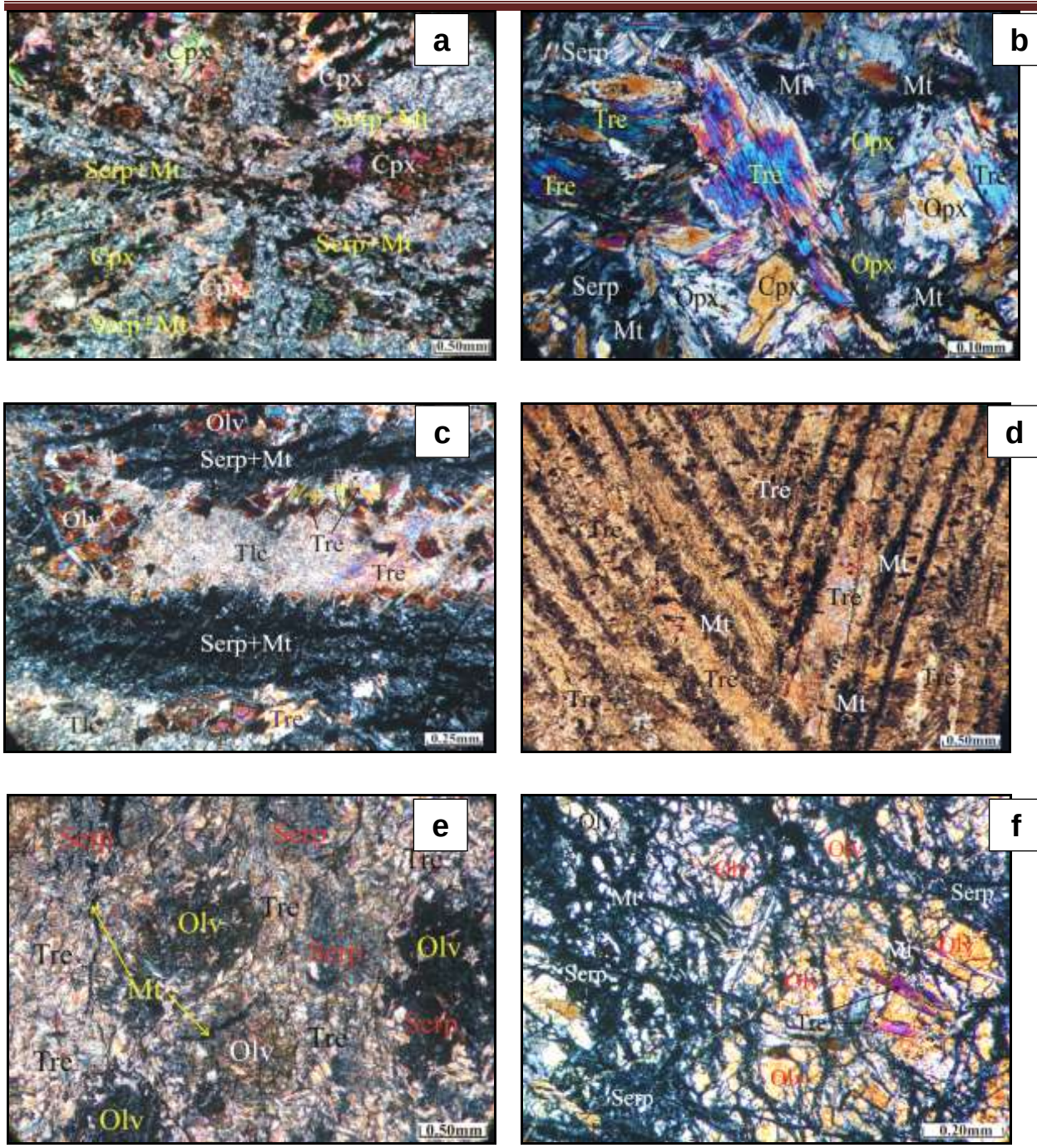

Fig.4. (a to d) Photomicrographs of spinifex zone. **(a)** Complete alteration of olivine and pyroxene to serpentine, magnetite, talc, tremolite and chlorite respectively. **(b)** Criss-cross arrangement of tremolite needles. **(c & d)** Alternate plates of pyroxene (altered to tremolite and chlorite) and olivine (altered to serpentine, magnetite and talc). **(e)** Cumulate zone display cumulus and inter-cumulus phases. (**f)**) Mesh texture formed due to the breakdown of olivine is a felty mass of serpentine and magnetite.
Abbreviations: Olv, Olivine; Serp, Serpentine; Mt, Magnetite; Tre, Tremolite; Cpx, Clinopyroxene; Opx, Orthopyroxene; Tlc, Talc

Geochemistry of komatiite

Nine representative samples of Kapili komatiite from the BGGB were analysed for major oxides by X-Ray Fluorescene (XRF) and trace elements and REE by Inductively Coupled Plasma Mass Spectrometer (ICP-MS) at Geological Survey of India, Eastern Region Laboratory, Kolkata, India. The analytical data is presented in the Table 1.

Major oxides and trace elements

All the analyzed samples fall within 'komatiite' field (Fig.5a) except one sample falls in the komatiite basalt field in CaO-MgO-Al_2O_3 triangular diagram after Viljoen et al., 1982. They are mantle-derived fractionates, as indicated from their plots in R_1-R_2 diagram (Fig.5b). Arndt, 2003 and Arndt et al., 2008 proposed three types of komatiites based on following parameters: (i) the Barberton type komatiites characterised by high CaO/Al_2O_3 (>1.0), low Al_2O_3/TiO_2 (<16) and depleted HREE; (ii) the Munro type komatiites with lower CaO/Al_2O_3 (<1.0), higher Al_2O_3/TiO_2 (>20) and HREE; and (iii) the Gorgana type komatiites with high Al_2O_3/TiO_2. Composition of Kapili komatiite has been compared with other komatiites in the world in different major element plots (Fig.6a-c) which clearly show the compositional resemblance between the Kapili komatiite and Barberton komatiite.

Kapili komatiites are relatively rich in SiO_2 contents (37-47%), similar to Barberton komatiites (Fig.6a), although silica enrichment during alteration may also have occurred because the rocks are quite altered. MgO content of basal cumulate rocks vary from 30.50 to 36.8% with lower MgO content from 20.62 to 29.18% in spinifex zone. The Al_2O_3/TiO_2 ratio varies between 8.7-30.5 in the spinifex zone and 8.2 to 28.1 in the cumulate zone. This ratio in the cumulate zone is significantly higher compared to Al-depleted Barberton komatiites (Al_2O_3/TiO_2: 10-15, Arndt et al., 2008). The range of CaO/Al_2O_3 ratio (0.73-1.82) is comparable with the Barberton komatiites (Lahaye and Arndt, 1996; Arndt et al., 2008). The large observed variation of LOI content (4.07-10.45 wt%) is due to the variable proportions of secondary phases e.g., tremolite, serpentine and chlorite which indicates the rocks have been suffered during metamorphism.

In the binary variation diagrams of major oxides and trace elements shows strong negative correlation between MgO versus, SiO_2, CaO, Al_2O_3, Na_2O, TiO_2, Cu, Sc and V plots (Fig.7). The strong linear correlations may be due to the effect of periodic removal of the cumulus phase from the melt. LOI shows strong positive correlation with MgO and CaO, possibly a mark of susceptibility to alteration of Mg-Ca-rich minerals to secondary hydrous phases (Fig.7). Apart from these, Co, Cr and Ni are also displayed a positive correlation against MgO (Fig.7). All the analysed samples of komatiites show a large range of variation in ΣREE (9.67 to 32.48ppm). Chondrite normalised REE fractionation patterns (Fig.8a) reveal a slight enrichment of LREE compared with HREE anomalies (Table 1). Komatiites show wide variation in ratios of $(Gd/Yb)_N$: (0.79-2.65) and $(La/Sm)_N$: (0.85-2.82). The average value of $(Gd/Yb)_N$ is 1.70 which is comparable with Barberton komatiites (>1). The primitive-mantle normalised multi-element spider diagrams (Fig.8b) display positive U, Pb and Y anomalies. Major element ratios such as CaO/Al_2O_3 and Al_2O_3/TiO_2 (Fig.9a&b) in combination with $(Gd/Yb)_N$ values have been used to understand the nature of mantle source and garnet fractionation (Jahn et al., 1982; Arndt, 2003).

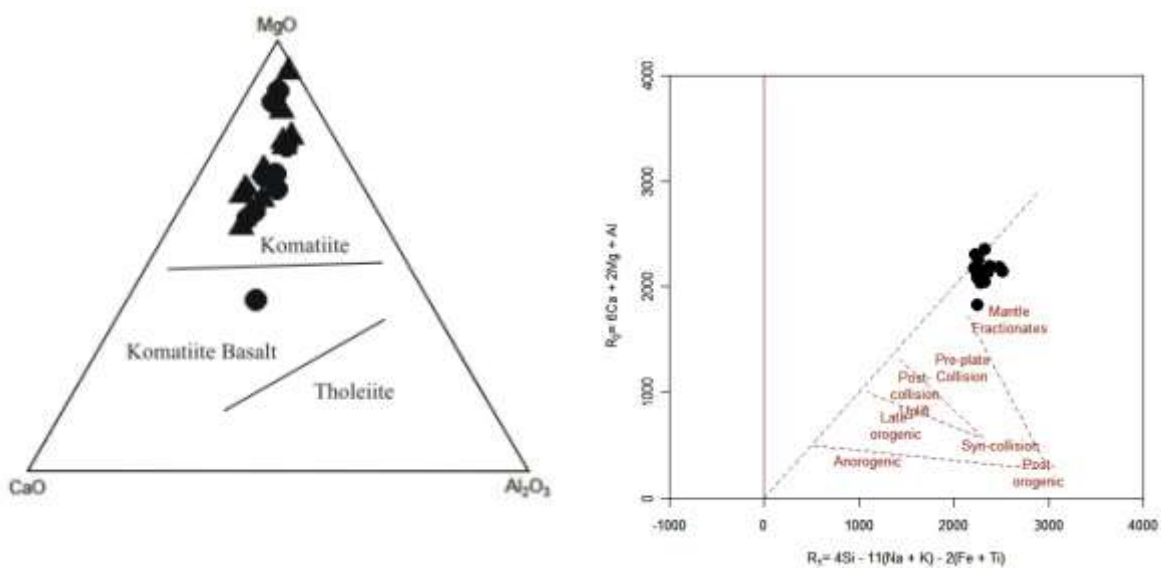

Fig.5. (a) Plots in the CaO-MgO-Al_2O_3 diagram (Viljoen et al., 1982). (● Kapili Komatiite; ▲ Komatiite data after Yadav et al., 2015). **(b)** Diagram of R_1=4Si-11(Na+K)-2(Fe+Ti) vs. R_2= 6Ca+2 Mg+Al (after Batchelor & Bowden, 1985) indicating Kapili komatiites are mantle derived fractionates.

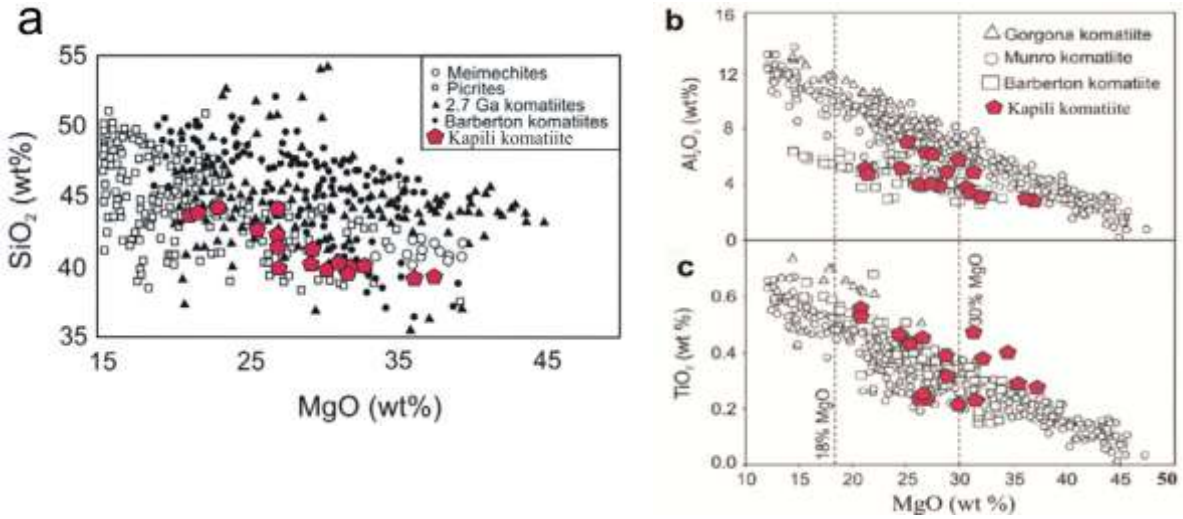

Fig.6. (a) MgO (wt%) vs. SiO_2 (wt%) plot of picrites, meimechites and komatiites of Barberton (data from Clarke, 1970; Pedersen, 1985; Arndt et al., 2008, and reference therein, GEOROC database *http://georoc.mpch-mainz.gwdg.de/georoc)*and komatiite of Kapili. **(b)** Plots of MgO (wt%) vs. Al_2O_3 and **(c)** MgO (wt%) vs. TiO_2 (wt%) of Gorgona, Munro, Barberton (data from Clarke, 1970; Pedersen, 1985; Arndt et al., 2008) and Kapili komatiite (this work).

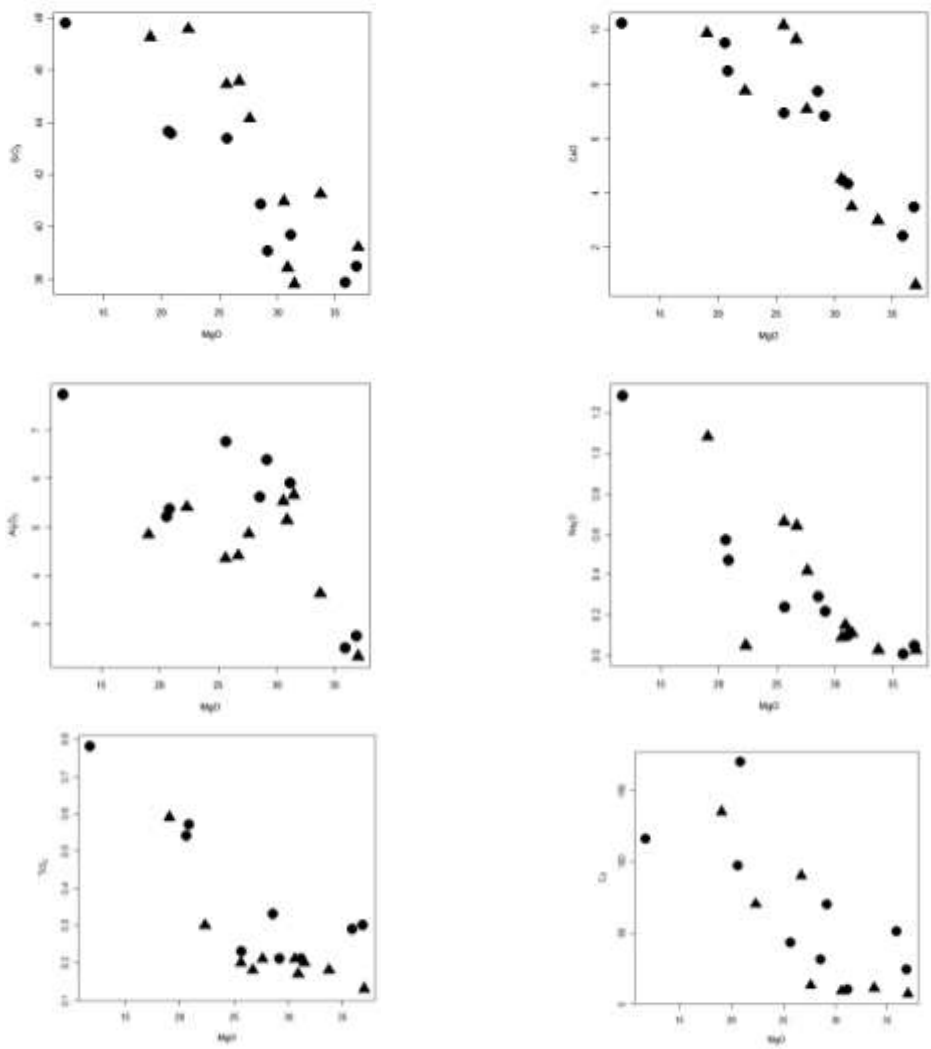

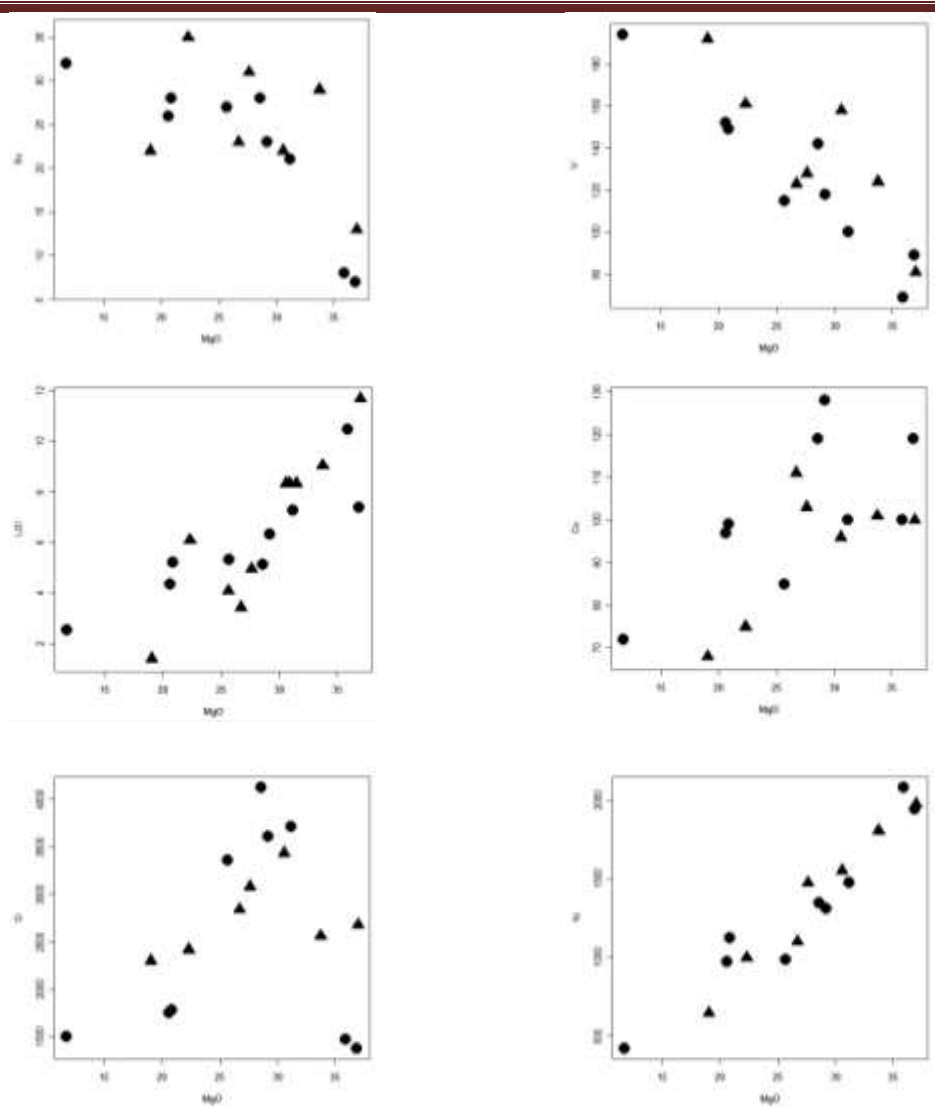

Fig.7. Plots of Kapili komatiites in variation diagrams for selected major oxides and trace elements plotted against MgO. (● Kapili Komatiite; ▲ Komatiite data after Yadav et al., 2015)

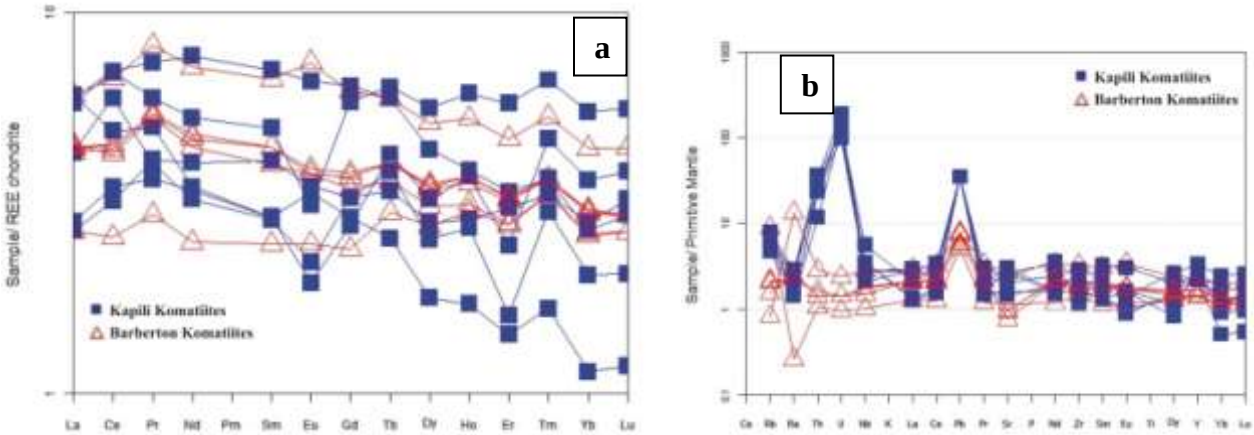

Fig.8. (a) Chondrite normalised REE plots of komatiites from Kapili and Barberton (Nakumura, 1974). **(b)** Primitive mantle normalized multi-element diagram of Kapili and Barberton komatiites (Sun and McDonough, 1989). Barberton komatiites data after Parman et al., 2003.

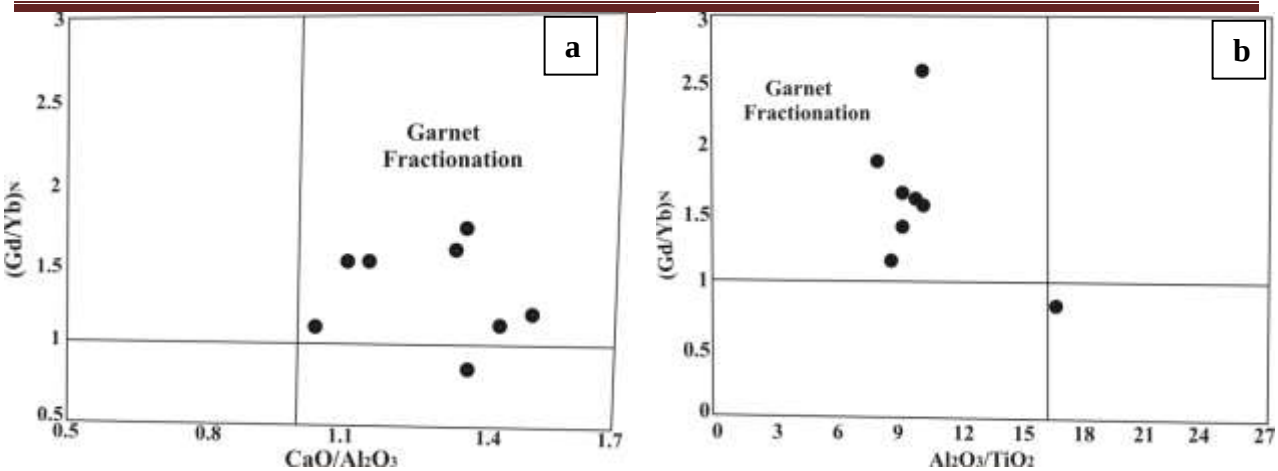

Fig. 9. (a & **b)** $(Gd/Yb)_N$ ratios vs. CaO/Al_2O_3 and Al_2O_3/TiO_2 plots of Kapili komatiites mostly samples come in garnet fractionation field (Jahn et al.,1982; Arndt, 2003).

Table. 1: Major and trace elements data of komatiites and komatitic basalt from Badampahar-Gorumahisani greenstone belt, Singhbhum craton

Sample No.	K1	K2	K3	K5	K6	K10	K15	K16	K7
SiO_2	43.57	43.65	38.48	40.86	39.06	39.68	43.37	37.86	47.79
Al_2O_3	5.37	5.21	2.75	5.62	6.38	5.91	6.75	2.51	7.72
Fe_2O_3	14.86	14.71	10.63	10.75	11.04	11.10	10.79	10.34	17.24
MnO	0.20	0.20	0.18	0.22	0.24	0.18	0.19	0.21	0.22
MgO	20.85	20.62	36.87	28.60	29.18	31.18	25.66	35.89	11.75
CaO	8.48	9.50	3.48	7.73	6.84	4.31	6.93	2.40	10.23
Na_2O	0.47	0.57	0.05	0.29	0.22	0.10	0.24	0.01	1.28
K_2O	0.06	0.05	0.01	0.03	0.03	0.03	0.02	0.01	0.10
TiO_2	0.57	0.54	0.30	0.33	0.21	0.21	0.23	0.29	0.78
P_2O_5	0.03	0.04	0.03	0.02	0.03	0.04	0.01	0.04	0.05
LOI	5.21	4.34	7.38	5.11	6.33	7.27	5.33	10.45	2.54
Total	99.67	99.43	100.16	99.56	99.56	100.01	99.52	100.01	99.70
Ba	28	34	20	10	69	15	20	20	20
Co	99	97	119	119	128	100	85	100	72
Cr	1782	1755	1377	4125	3611	3712	3359	1475	1503
Cu	170	97	24	31	70	10	43	51	116
Ga	12	11	9	10	9	10	11	9	13
Nb	5	5	2.5	2	0.9	1.5	3.4	4.1	3
Ni	1124	972	1943	1344	1307	1476	983	2079	419
Pb	<5	<5	<5	<5	<5	<5	<5	<5	5
Rb	5	7	5	5	8	5	2.7	3	6
Sc	28	26	7	28	23	21	27	8	32
Th	1	2.2	3.1	1	3.1	3	2.6	2.9	2
U	2	3	2.3	2.7	1.5	4	3.5	3	3.5

Sr	70	39	34	64	62	51	38	5	51
V	149	152	89	142	118	100	115	69	194
Y	15	14	10	12	10	11	13	11	19
Zn	66	82	57	62	52	58	55	61	85
Zr	50	39	18	30	19	13	32	18	59
La	2.59	3.48	0.93	2.01	5.16	1.96			3.18
Ce	6.42	6.59	3.02	4.23	11.83	6.07			10.82
Pr	0.92	0.85	0.41	0.56	1.24	0.83			1.46
Nd	4.98	3.21	2.15	2.2	4.75	4.86			7.19
Sm	1.48	0.77	0.59	0.59	1.15	1.44			2.03
Eu	0.37	0.12	0.26	0.15	0.24	0.51			0.59
Gd	2.03	0.75	0.8	0.76	1.15	1.77			2.11
Tb	0.35	0.15	0.12	0.2	0.23	0.28			0.41
Dy	1.9	0.66	0.61	1.11	1.14	1.5			2
Ho	0.37	0.11	0.12	0.26	0.25	0.27			0.42
Er	1.23	0.26	0.32	0.55	0.55	0.76			0.85
Tm	0.18	0.06	0.05	0.14	0.14	0.11			0.2
Yb	1.14	0.38	0.25	0.8	0.75	0.59			1.06
Lu	0.19	0.05	0.04	0.13	0.13	0.1			0.16
ΣREE	24.15	17.44	9.67	13.69	28.71	21.05			32.48
Fe_2O_3/ (Fe_2O_3+MgO)	0.42	0.42	0.22	0.27	0.27	0.26	0.3	0.22	0.59
Al_2O_3/ TiO_2	9.4	9.7	9.2	17	30.4	28.1	29.3	8.7	9.9
CaO/Al_2O_3	1.58	1.82	1.27	1.37	1.07	0.73	1.03	1	1.33
Nb/U	2.5	1.67	1.09	0.74	0.6	0.38	0.97	1.37	0.86
Nb/Th	5	2.27	0.81	2	0.29	0.5	1.35	1.41	1.5
Zr/Nb	10	7.8	7.2	15	21.11	8.77	9.4	4.39	20.01
Nb/Y	0.33	0.36	0.25	0.17	0.09	0.14	0.26	0.37	0.16
Zr/Y	3.33	2.79	1.8	2.5	1.9	1.18	2.46	1.64	3.11
Nb/La	1.93	1.44	2.69	1	0.17	0.77			0.94
(Zr/Sm)Pm	1.34	2.01	1.21	2.01	0.66	0.36			1.15
(La/Yb)N	1.57	6.35	2.59	1.74	4.77	2.3			2.08
(La/Sm)N	1.09	2.82	0.99	2.13	2.81	0.85			0.98
(Gd/Yb)N	1.47	1.63	2.65	0.79	1.27	2.48			1.65

Discussion

Effects of alteration and metamorphism

The petrographic evidence presented above suggests that the Kapili komatiites have experienced several episodes of post-igneous recrystallization and metamorphism. The studied komatiites comprising mainly serpentine, tremolite, chlorite, talc, chromite and secondary magnetite have been attributed greenschist to lower amphibolite facies of metamorphism. At places, rarely preserved primary olivine and clinopyroxenes within this rock. Olivine, clinopyroxene and minor amounts of chromite are the only liquidus minerals found in komatiites. Thus the effect of crystal fractionation in komatiites is to produce very simple chemical trends for all elements. Formation of secondary minerals like serpentine from olivine and tremolite from clinopyroxene requires gain/loss of MgO and SiO_2 to the bulk rock. Negative trends

between MgO vs. SiO_2 (Fig.7) indicating modification of MgO and/or SiO_2 by secondary processes. Plot of MgO vs. CaO (Fig.7) display negative correlation might be due to relative gain of CaO and loss of MgO during late alteration and metamorphism. Primitive mantle normalised multielement spider diagrams display criss-crossing of LILE indicative of their mobility. This result is also supported by smooth fractionation patterns of major element oxides viz. SiO_2, CaO, Al_2O_3, Na_2O, TiO_2 and LOI plotted against MgO.

The causes of alteration of komatiites in Archaean greenstone belts may be chemically altered during sea-floor hydrothermal alteration following by their eruption and later metamorphic recrystallization. In this study there is petrographic evidence for two stages of alteration and metamorphism. The earliest alteration event is the serpentinisation of olivine in the komatiites was followed by the development of tremolites porphyroblasts. These observations suggest that the komatiites experienced an early alteration event during which olivine was serpentinised and become Fe-rich and during which chlorite formed. Relict inclusions of clinopyroxenes are preserved within tremolite which suggests the formation of tremolites from clinopyroxenes. Later recrystallization, correlated with the regional metamorphism and deformation of the greenstone belt, let to the growth of serpentine and tremolite in the komatiites.

Al-depletion and garnet fractionation

Komatiites are mainly categorised on Al content viz. Al-depleted Barberton komatiites and Al-enriched Munro komatiites. The genesis of Al-depleted komatiite is explained by melting of mantle at greater depth in the presence of garnet in the melt phase (Jahn et al., 1982; Arndt, 2003) as in the Barberton komatiites. The origin of Al-enriched Munro komatiites is inferred to be by a high degree (~50%) of peridotite melting at shallower level, where the mantle source intersected the solidus and garnet was removed from the residue before the melt acquired komatiitic composition. Jahn et al., 1982 and Gruau et al., 1992 have been used CaO/Al_2O_3 ratios and $(Gd/Yb)_N$ values to constrain the source characteristics, particularly garnet fractionation or retention in the source. High CaO/Al_2O_3 (>1.0) and $(Gd/Yb)_N$ >1.0 are considered indicative of the presence of garnet as residual phase in the mantle, and low CaO/Al_2O_3 (<1.0) and $(Gd/Yb)_N$ <1.0 suggestive of garnet entering into the melt phase.

Kapili komatiites samples are characterised by Al-depletion with high CaO/Al_2O_3 ratios (>1.0), Al_2O_3/TiO_2 (8-30) and $(Gd/Yb)_N$ >1.0 implying involvement of garnet as a residual phase. Samples with high MgO contents generally display CaO/Al_2O_3 ratios >1.0, whereas samples with low MgO contents have low CaO/Al_2O_3 ratios <1.0. Major element ratios such as CaO/Al_2O_3 and Al_2O_3/TiO_2 in combination with $(Gd/Yb)_N$ values have been used to understand the nature of mantle sources and garnet fractionation (Jahn et al., 1982; Arndt, 2003). In this study bivariate plots of $(Gd/Yb)_N$ versus CaO/Al_2O_3 and Al_2O_3/TiO_2 (Fig.9a&b) suggest varying degree of involvement of garnet in the generation of komatiite melt in the mantle.

Affinities between Kapili komatiite and Barberton komatiite

The komatiites are quite enriched in SiO_2 and MgO; depleted in Al_2O_3 and higher TiO_2 with significantly higher Al_2O_3/TiO_2 and CaO/Al_2O_3 ratios indicating resemblance with the Barberton komatiite (Arndt et al., 2008; Robin- Popieul et al., 2012). Earlier researchers have proposed a subduction-accretion complex in the Singhbhum craton during Palaeo-Mesoarchaean time (Mukhopadhyay et al., 2012; Prabhakar and Bhattacharya, 2013). Although the precise age of the Kapili komatiite in the Singhbhum craton is hitherto unknown, intrusion of 3.2Ga Singhbhum granodiorite (Reddy et al., 2009) constrains the upper age limit of the komatiite. Earlier researchers reveal significant crust forming events around 3.3-3.4Ga in the Singhbhum craton (Sharma et al., 1994; Saha, 1994; Mukhopadhyay, 2001; Tait et al., 2011). Jayananda et al., 2008 suggested that the komatiite volcanism and subcontemporaneous mafic to felsic volcanism and granitoid plutonism in the surrounding TTG basement in the Western Dharwar craton can be best explained by a mantle plume-arc model. Sharma et al., 1994 suggested the growth of continental crust in the Singhbhum craton during the Mesoarchaean time occurred in response to magmatic under plating in a plume setting. The ultramafic sequences in the BGGB contain pillow lava and amygdules indicating to their eruption in marine and sub-aerial environments.

The majority of Kapili komatiites show high contents of MgO, Ni, Cr and Al-depletion and no Nb anomalies consistent with their generation in a deep mantle hot spot environment associated with a rising plume. The observed geochemical characteristics together with high melt temperatures and great depth of melt generation of the studied komatiites favour a mantle plume setting for their origin. Therefore, the plume model alone does not account for the formation of sub-contemporaneous TTG basement. So, a combined mantle plume-arc model can be considered to explain litho-assemblages of BGGB and accretion of TTG during the Mesoarchaean in the Singhbhum craton.

Table 2: Comparison parameters of Kapili komatiite and Barberton komatiite (Parman et al., 2003; Arndt et al., 2008)

Parameter	Kapili Komatiite	Barberton Komatiite
Flow characteristics	Random spinifex, platy spinifex and cumulate zones	Random spinifex, platy spinifex and cumulate zones
Mineralogy		
Primary minerals	Olivine, Augite, Enstatite, Magnetite, Chromite	Olivine, Augite, Orthopyroxene, Glass, Spinel, Magnetite, Chromite
Secondary minerals	Serpentine, Tremolite, Chlorites, Talc, Secondary Magnetite	Serpentine, Tremolite, Chlorites, Talc, Secondary Magnetite, Epidote
Geochemistry		
SiO_2	38.48 - 47.79 wt%	45.8 - 50.4 wt%
Al_2O_3	2.51 - 6.75 wt%	2.5 - 4.5 wt%
MgO	20.62 - 36.87 wt%	24.3 - 36.3 wt%
CaO	2.40 - 9.50 wt%	3.37 - 9.51 wt%
TiO_2	0.21 - 0.57 wt%	0.22 - 0.41 wt%
Cr	1377 - 4125 ppm	1640 - 5441 ppm
Ni	419 - 2079 ppm	1067 - 2165 ppm
CaO/Al_2O_3	0.73 - 1.82	1 - 2.8
Al_2O_3/TiO_2	8 - 30	8 - 18
∑REE	9.67 - 28.71 ppm	7.85 - 21.66 ppm
$(La/Sm)_N$	0.85 -2.82	0.80 - 1.2
$(Gd/Yb)_N$	0.79 - 2.65	0.90 - 1.4
$(La/Yb)_N$	1.57 - 6.35	1.0 - 1.7

Conclusions

The Kapili komatiite of Badampahar-Gorumahisani greenstone belts shows petrogenetic affinity with Barberton komatiite. The komatiites display well preserved random spinifex, platy spinifex and cumulate zones. Petrographic studies reveal the mineral assemblage of tremolite, actinolite, serpentine, chlorite and talc indicates of greenschist to lower amphibolite facies of metamorphism. The komatiites are relatively enriched in SiO_2 (38.48-47.79 wt%) and MgO (20.62-36.87 wt%); depleted in Al_2O_3 (2.51-6.75 wt%) and TiO_2 (0.21-0.57 wt%) with significantly higher Al_2O_3/TiO_2 (8.7-30.4), CaO/Al_2O_3 (0.73- 1.82), $(Gd/Yb)_N$ (0.79-2.65), $(La/Yb)_N$ (1.57-6.35), $(La/Sm)_N$ (0.85-2.82) and $(Zr/Sm)_{PM}$ (0.36-2.01) ratios indicating resemblance with the Barberton komatiite. The element characteristics of these komatiites indicate derivation of parent magma in a mantle plume-arc geodynamic setting during the Mesoarchean in the Singhbhum Craton with moderate contamination by continental crust.

Acknowledgements

The author thanks the Director General, Geological Survey of India for permitting publication of the paper. He is also indebted to Dr. H. Sarvothaman, D. K. Rai, and V. Devdas, Geological Survey of India for their technical guidance during the work.

References

1. Allegre, C.J., 1982: Genesis of Archaean komatiites in a wet ultramafic subducted plate. In: Arndt NT, Nisbet EG (eds) Komatiites. Springer-Verlag, Berlin, pp 495-500.
2. Arndt, N.T., 2003: Komatiites, kimberlites, and boninites. J. Geophys. Res.108, 2293.
3. Arndt, N.T., Ginibre, C., Chauvel, C., Albarede, F., Cheadle, M., Herzberg, C., Jenner, G., and Lahaye, Y., 1998: Were komatiites wet? Geology 26: 739-742.
4. Arndt, N.T. and Nisbet, E.G., 1982: What is a komatiite? In: Arndt, N.T., Nisbet, E.G. (Eds.), Komatiites. George Allen and Unwin, London, pp. 19-28.
5. Arndt, N.T., Lesher, C.M., and Barnes, S.J., 2008: Komatiite. Cambridge University Press.
6. Batchelor, R.A. and Bowden, P., 1985: Petrogenetic interpretation of granitoid rock series using multicationic parameters. Chemical Geology, 48, 43-55.
7. Boehler, R., Chopelas, A., and Zerra, A., 1995: Temperature and chemistry of the core-mantle boundary. Chem. Geol. 120: 199-205.

8. Chaudhuri, T., Mazumder, R., and Arima, M., 2015: Petrography and geochemistry of Mesoarchaean komatiites from the eastern Iron Ore belt, Singhbhum craton, India, and its similarity with 'Barberton type komatiite'. Jour. Africa. Earth Sci. (101) 135-147.
9. Clarke, D.B., 1970. Tertiary basalts of Baffin Bay: possible primary magma from the mantle. Contrib. Miner. Petrol. 25, 203-224.
10. Goswami, J.N., Mishra, S., Wiedenbeck, M., Ray, S.L., and Saha, A.K., 1995: 207Pb/206Pb ages from the OMG, the oldest recognized rock unit from Singhbhum-Orissa Iron Ore craton, E. India. Curr. Sci. 69, 1008-1012 (Bangalore).
11. Green, D.H., 1975: Genesis of Archaean peridotitic magmas and constraints on Archaean geothermal gradients and tectonics. Geology 3, 15-18.
12. Grove, T.L., and Parman, S. W., 2004: Thermal evolution of the earth as recorded by komatiites. Earth Planet Sci. Lett. 219: 173-187.
13. Gruau, G., Toupin, S., Fourcade, S., Blais, S., 1992: Loss of (Nd, O) and chemical (REE) memory during metamorphism of komatiites: new evidence from eastern Finland. Contribution to Mineralogy and Petrology 112, 66-82.
14. Herzberg, C., 1995: Generation of plume magmas through time: an experimental perspective. Chem. Geol. 126, 1-16.
15. Jahn, B.M., Gruau, G., and Glickson, A.Y., 1982: Komatiites of the Onverwacht Group, South Africa: REE chemistry, Sm–Nd age and mantle evolution. Contrib. Miner. Petrol. 80, 25-40.
16. Jayananda, M., Kano, T., Peucat, J.J., and Channabasappa, S., 2008: 3.35Ga komatiite volcanism in the western Dharwar craton, southern India: constraints from Nd isotopes and whole-rock geochemistry. Precambr. Res. 162, 160-179.
17. Lahaye, Y., and Arndt, N.T., 1996: Alteration of a komatiitic flow: Alexo, Ontario, Canada. J. Petrol. 37, 1261-1284.
18. Misra, S., Deomurari, M.P., Wiedenbeck, M., Goswami, J.N., Ray, S., and Saha, A.K., 1999: $^{207}Pb/^{206}Pb$ zircon age ages and the evolution of the Singhbhum craton, eastern India: an ion microprobe study. Precambrian Research 93, 139-151.
19. Misra, S., 2006: Precambrian chronostratigraphic growth of Singhbhum-Orissa Craton, eastern Indian Shield: an alternative model. J. Geol. Soc. India, 67, 356-378.
20. Mukhopadhyay, D., 2001: The Archean nucleus of Singhbhum: the present state of knowledge. Gondwana Res. 4, 307-318.
21. Mukhopadhyay, J., Ghosh, G., Zimmermann, U., Guha, S., Mukherjee, T., 2012: A 3.51Ga bimodal volcanics-BIF-ultramafic succession from Singhbhum Craton: implications for Palaeoarchaean geodynamic processes from the oldest greenstone succession of the Indian subcontinent. Geol. J. 47, 284-311.
22. Nakamura, N. 1974: Determination of REE, Ba, Fe, Mg, Na and K in carbonaceous and ordinary chondrites, Geochim. et Cosmochim. Acta, 38, 757-775.
23. Ohtani, E., Kawabe, I., Moriyama, J., and Nagata, Y., 1989: Partitioning of elements between majorite garnet and melt and implications for petrogenesis of komatiite. Contrib. Miner. Petrol. 103, 263-269.
24. Parman, S.W., Timothy, N.S., Grove, L. and Dann, J.C., 2003: Constraints on the pre-metamorphic trace element composition of Barberton komatiites from ion probe analyses of preserved clinopyroxene. Contrib. Mineral Petrol 144: 383-396.
25. Pedersen, A.K., 1985: Reaction between picritic magma and continental crust: early Tertiary silicic basalts and magnesian andesites from Disko, West Greenland. Bull. Geol. Soc. Greenland 152, 126.
26. Prabhakar, N. and Bhattacharya, A., 2013: Paleoarchean partial convective overturn in the Singhbhum Craton, eastern India. Precambr. Res. 231, 106-121.
27. Reddy, S.M., Clarke, C. and Mazumder, R., 2009: Temporal constraints on the evolution of the Singhbhum Crustal Province from U-Pb SHRIMP data. In: Saha, D. & Mazumder, R. (Eds.) Paleoproterozoic Supercontinents and Global Evolution. International Conference on Paleoproterozoic Supercontinents and Global Evolution Abstract Volume. International Association for Gondwana Research, Conference Series 9, 17-18.
28. Robin-Popieul, C.C.M., Arndt, N.T., Chauvel, C., Byerly, G.R., Sobolev, A.V. and Wilson, A., 2012: A new model for Barberton komatiites; deep critical melting with high melt retention. J.Petrol.53, 2191-2229.
29. Saha, A.K., 1994: Crustal evolution of Singhbhum-North, Orissa, eastern India. Geol. Soc. India Mem., 27.

30. Sahu, N.K., and Mukherjee, M.M., 2001: Spinifex Textured Komatiite from Badampahar-Gorumahisani Schist Belt, Mayurbhanj District, Orissa. Jour. Geol. Soc. India, 57, pp 529-534.
31. Sharma, M., Basu, A.R. and Ray, S.L., 1994: Sm-Nd isotopic and geochemical study of the Archean tonalite-amphibolite association from the eastern India craton. Contrib. Mineral. Petr. 117, 45-55.
32. Subba Rao, D.V., and Naqvi, S.M., 1999: Archaean Komatiites from the older schist belt of Kalyadi in Western Dharwar craton, Karnataka. J. Geol. Soc. India, 53, 347-354.
33. Sun, S.S., and McDonough, W.F., 1989. Chemical and isotopic systematics of oceanic basalts: implications for mantle composition and processes. In: Saunders, A.D., Norry, M.J. (Eds.), Magmatism in the Ocean Basins, vol. 42. Geological Society, London, pp. 313-345 (Special Publications).
34. Tait, J., Zimmermann, U., Miyazaki, T., Presnyakov, S., Chang, Q., Mukhopadhyay, J., and Sergeev, S., 2011: Possible juvenile Palaeoarchaean TTG magmatism in eastern India and its constraints for the evolution of the Singhbhum craton. Geol. Mag.148 (2), 340-347.
35. Tushipokla, and Jayananda, M. 2013: Geochemical constraints on komatiite volcanism from Sargur Group Nagamangala greenstone belt, western Dharwar craton, southern India: Implications for Mesoarchean mantle evolution and continental growth. Geosci. Fron. 4, 321-340.
36. Viljoen, M.J., and Viljoen, R.P., 1969a: Archaean volcanity and continental evolution in the Barberton region, Transvaal. In: Clifford, T.N., Gass, I. (Eds.), African Magmatism and Tectonics. Oliver and Boyd, Edinburgh, pp. 27-39.
37. Viljoen, M.J., Viljoen, R.P., and Pearton, T.N., 1982: In Arndt, N. T., Nisbet, E. G. (Eds.), the Nature and Distribution of Archaean Komatiite Volcanics in South Africa. Komatiites, Allen and Unwin, London, pp. 53-79.
38. Xie, Q., Kerrich, R., and Fan, J., 1993: HFSE/REE fractionations recorded in three komatiite-basalt sequences, Archean Abitibi greenstone belt: implications for multiple plume sources and depths. Geochim. Cosmochim. Acta 57, 4111-4118.
39. Yadav, P.K., Pradhan, U.K., Mukherjee, A., Sar, R.N., Sahoo, P., and Das, M., 2015: Basic characterization of Kapili Komatiite from Badampahar-Gorumahisani Schist Belt, Singhbhum Craton, Odisha, Indian Jour. Geosci. India, 69 (1), 1-12.
40. Yadav, P.K., Sahoo, P., Pradhan, U.K., and Das, M., 2016: Komatiite from Mesoarchaean Badampahar-Gorumahisani greenstone belt, Singhbhum craton, eastern India: Petrogenetic affinity with 'Barberton type'. 35th Inter. Geol. Congress., Cape5 Town, South Africa. Paper No.671.
41. Yadav, P.K., and Das, M., 2017: Petrology, geochemistry and petrogenesis of Al-depleted komatiite from Badampahar-Gorumahisani Greenstone Belt of Eastern Iron Ore Group, Singhbhum Craton, Indian Jour. Geosci. India, 70 (3&4), 71 (1), 313-328.